

Hole localization in underdoped superconducting cuprates near $\frac{1}{8}$ doping

J. L. Cohn and C. P. Popoviciu

Department of Physics, University of Miami, Coral Gables, Florida 33124

Q. M. Lin and C. W. Chu

Texas Center for Superconductivity at University of Houston and the Department of Physics, University of Houston, Houston, Texas 77204

(Received 14 October 1998)

Measurements of thermal conductivity versus temperature over a broad range of doping in $\text{YBa}_2\text{Cu}_3\text{O}_{6+x}$ and $\text{HgBa}_2\text{Ca}_{n-1}\text{Cu}_n\text{O}_{2n+2+\delta}$ ($n=1,2,3$) suggest that small domains of localized holes develop for hole concentrations near $p=1/8$. The data imply a mechanism for localization that is intrinsic to the CuO_2 planes and is enhanced via pinning associated with oxygen-vacancy clusters. [S0163-1829(99)01805-6]

There has been considerable recent interest in novel charge- and spin-ordered phases which may compete with superconductivity in the cuprates.¹ This stripe order is favored at CuO_2 planar hole concentrations near $p=1/8$ for which the modulation wavelength is commensurate with the lattice, and when an appropriate pinning potential is present. Inelastic neutron scattering results² suggest that stripe modulations are disordered and/or fluctuating in $\text{La}_{1-x}\text{Sr}_x\text{CuO}_4$ (La-214) and $\text{YBa}_2\text{Cu}_3\text{O}_{6+x}$ (Y-123). Nuclear magnetic and quadrupole resonance (NMR and NQR) studies^{3,4} indicate the presence of localized holes in the CuO_2 planes. Whether localized holes are a general feature of cuprates and contribute to short-ranged charge/spin segregation and the normal-state pseudogap^{5,6} are fundamental issues of current interest.

Here we report the observation of anomalies at $p=1/8$ revealed in the oxygen doping dependence of thermal conductivity (κ) in Y-123 and Hg cuprates. Our principal finding is that a fraction of the doped holes in the CuO_2 planes become localized near this particular doping level. This fraction correlates with the oxygen vacancy concentration in the charge reservoir layers, consistent with the formation of nanoscale, hole-localized domains that are pinned near oxygen-vacancy clusters.

Two prominent characteristics of the in-plane heat conductivity in superconducting cuprates⁷ are a normal-state κ predominantly of lattice origin, and an abrupt increase in κ at $T \leq T_c$. To motivate our proposal that κ probes localized holes, we demonstrate for Y-123 that its magnitude and temperature derivative at T_c correlate with independent measures of local structural distortions (planar Cu NQR) and the superfluid fraction (specific heat jump), respectively, throughout the underdoped regime ($p \leq 0.16$). Consider data from previous work⁸ that illustrate the $p=1/8$ features in κ (Fig. 1). The upper panel shows normal-state data $\kappa(p, T=100\text{ K})$ for an Y-123 polycrystal and the ab plane of single crystals. The lower panel shows, for the same specimens, the dimensionless slope change in κ at T_c defined as⁸ $\Gamma \equiv -d(\kappa^s/\kappa^n)/dt|_{t=1}$, where $t=T/T_c$ and $\kappa^s(\kappa^n)$ is the thermal conductivity in the superconducting (normal) state. Γ measures the change in scattering of heat carriers (electrons and phonons) induced by superconductivity. Both quantities exhibit local minima near $p=1/8$.

Figure 1(a) implies a sharply reduced lattice conductivity

(κ_L) about $p=1/8$, since the electronic thermal conductivity (κ_e) at $T > T_c$ in optimally doped, single-crystal Y-123 represents only $\sim 10\%$ of the total $\kappa = \kappa_e + \kappa_L$.¹⁰ We attribute this suppression in κ_L to phonon scattering by local distortions of the CuO polyhedra. In support of this interpretation is the doping behavior of the relative intensity (I_{NQR}) of anomalous planar ^{63}Cu NQR peaks for Y-123, indicative of charge inhomogeneity in the planes, and attributed to the presence of localized holes.⁴ The simple assumption that the total thermal resistivity is a sum of a term proportional to this disorder ($\propto I_{\text{NQR}}$), and a constant term from other scattering, reproduces $\kappa(p)$ quite well [crosses, Fig. 1(a)]. Studies of κ in lightly doped insulating cuprates and structurally similar

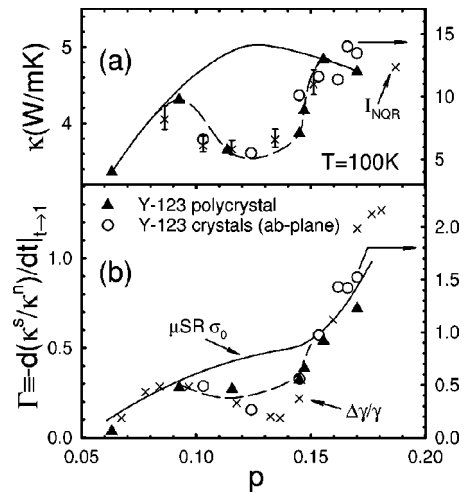


FIG. 1. (a) Doping dependence of the normal-state κ at $T = 100\text{ K}$ for Y-123 polycrystals and the ab plane of single crystals from Ref. 8. Values of p were determined from thermopower measurements following Ref. 9. Also plotted (\times 's, right ordinate) is $(0.08 + 0.16I_{\text{NQR}})^{-1}$, where I_{NQR} is the anomalous planar ^{63}Cu NQR signal (Ref. 4, see text). The dashed curve is a guide to the eye. The solid curve is discussed in the text. (b) The normalized slope change in $\kappa(T)$ at T_c vs doping for each of the Y-123 specimens in (a). Also shown are the normalized electronic specific heat jump $\Delta\gamma/\gamma$ from Ref. 5 (\times 's), and the μSR depolarization rate (in μs^{-1}) from Ref. 12 (solid curve), divided by 1.4 and 2.7, respectively, and referred to the right ordinate. The dashed curve is described in the text.

manganites¹¹ provide further evidence that bond disorder associated with localized charge is an effective phonon scattering mechanism in perovskites.

The electronic specific heat jump for Y-123,⁵ $\Delta\gamma/\gamma(p)$ [crosses, Fig. 1(b)], correlates remarkably with $\Gamma(p)$. Though the origin of the slope change in κ at T_c (i.e., electronic or phononic) has been a subject of some debate, this correlation demonstrates unambiguously that Γ , similar to $\Delta\gamma/\gamma$, measures the difference between the normal- and superconducting-state low-energy electronic spectral weight. This conclusion is robust since the correlation holds for both polycrystals and single crystals; in spite of additional thermal resistance due to c -axis heat flow and granularity in the polycrystal, changes with doping reflect the intrinsic behavior of the in-plane heat conduction.

The muon spin rotation (μ SR) depolarization rate (σ_0),¹² a measure of the superfluid density, matches the data for Γ and $\Delta\gamma/\gamma$ at $p < 0.09$ and $p > 0.15$ when suitably scaled [solid curve in Fig. 1(b)]. The sharp rise in σ_0 for $p > 0.15$ is due to the superconducting condensate on oxygen-filled chains.¹² The range of p over which Γ and $\Delta\gamma/\gamma$ deviate from the μ SR curve coincides with the range of suppressed κ . The suppressed transfer of spectral weight below T_c is consistent with the localization of a fraction of planar holes. That σ_0 is not also suppressed near $p = 1/8$ indicates that hole-localized domains do not inhibit the formation of a flux lattice in adjacent regions where holes are itinerant. The scenario we have outlined resolves the prior inconsistency of the nonmonotonic $\Delta\gamma/\gamma$ doping behavior with the continuously rising pseudogap energy scale, inferred from numerous experiments in the underdoped regime.^{5,6}

If our interpretation is correct the maximum density of localized holes occurs at $p = 1/8$. This suggests a possible connection with the physics of stripe formation and raises questions about the generality of this phenomenon and the role of oxygen vacancies. To address these issues we have studied κ in $\text{HgBa}_2\text{Ca}_{m-1}\text{Cu}_m\text{O}_{2m+2+\delta}$ [Hg-1201 ($m=1$), Hg-1212 ($m=2$), Hg-1223 ($m=3$)]. A single HgO_δ layer per unit cell contributes charge to m planes in Hg-12($m-1$) m so that the oxygen vacancy concentration $1-\delta$ increases with decreasing m [at optimum doping, $\delta_{opt} \approx 0.18$ (Hg-1201), 0.35 (Hg-1212), and 0.41 (Hg-1223) (Ref. 13)].

The preparation of the polycrystalline starting materials is described elsewhere.¹⁴ Transport measurements were performed on specimens ($\sim 1 \times 1 \times 3 \text{ mm}^3$) cut from as-prepared disks; each was measured repeatedly up to ten times after successive heat treatments at 300–350 °C in flowing argon or vacuum to reduce the oxygen content. The thermopower (S) and thermal conductivity were measured during each experimental run using 25 μm type- E thermocouples and a steady-state technique. Heat losses via radiation and conduction through the leads (10–15 % near 300 K and 1–3 % for $T < 120$ K) were determined in separate experiments and the κ data corrected. Uncertainty in the contact geometry introduces a $\pm 5\%$ inaccuracy in κ .

Figure 2 shows $S(T)$ and $\kappa(T)$ for the Hg-1212 specimen. The thermopower curves are labeled by p , as determined from $S(290 \text{ K})$ and the universal $S(p)$ relations established by Tallon *et al.*⁹ Data for Hg-1201 and Hg-1223 yield similar sets of curves. Figure 3 shows $T_c(p)/T_c^{\text{max}}$ for

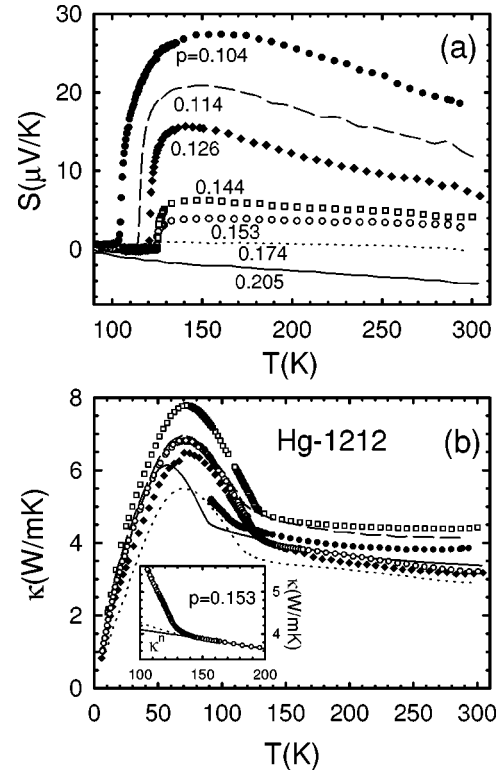


FIG. 2. (a) Thermoelectric power and (b) thermal conductivity vs temperature for Hg-1212. Data at $p = 0.121$ and $p = 0.132$ are omitted from both (a) and (b) for clarity. The inset shows $\kappa(T)$ near T_c and extrapolated κ^n curves for $p = 0.153$.

each of the materials studied. The data follow the generic high- T_c phase curve,⁹ approximated well by the parabolic form, $T_c(p)/T_c^{\text{max}} = 1 - 82.6(p - 0.15)^2$ (solid curve, Fig. 3).

The doping dependencies, $\kappa(p, T/T_c^{\text{max}} = 1.2)$ and $\Gamma(p)$ for each material are shown in Figs. 4(a) and 4(b), respectively. As for the Y-123 data,⁸ κ^n was determined by polynomial fits to the normal-state data at $t \geq 1.2$ (see inset, Fig. 2). Uncertainties in the heat-loss corrections and extrapolations of κ^n in the range $0.9 \leq t < 1.2$ are reflected in the error bars for Γ . Uncertainties in the extrapolations were established by varying the range of data and polynomial order used for fitting.

The data for the Hg materials are qualitatively similar to that of Y-123, but with the magnitude of suppression near

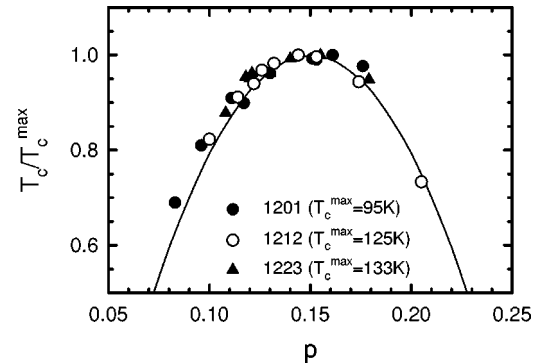


FIG. 3. $T_c(p)$ normalized to T_c^{max} for each of the Hg compounds. The solid curve is $T_c/T_c^{\text{max}} = 1 - 82.6(p - 0.15)^2$.

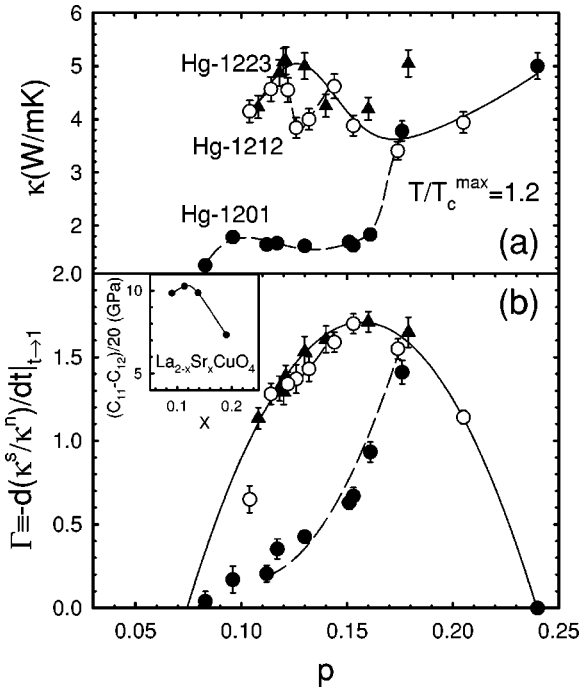


FIG. 4. (a) Doping dependence of the normal-state κ at $T/T_c^{\max} = 1.2$ for each of the Hg compounds. Dashed curves are guides to the eye and the solid curve is described in the text. (b) The normalized slope change in $\kappa(T)$ at T_c vs doping for each of the Hg compounds at the same doping levels as in (a). The solid line is $1.71 - 250(p - 0.157)^2$. Dashed curves are described in the text. The inset shows elastic constant data from Ref. 15.

$p = 1/8$ in κ and Γ increasing with the oxygen vacancy concentration. Consider first the $\Gamma(p)$ data for Hg-1223 which falls on an inverted parabola, centered near $p = 0.16$ [solid curve, Fig. 4(b)]. This behavior is similar to the μSR curve for Y-123, and suggests that the superconducting condensate is not suppressed in Hg-1223. An extension of our interpretation for Y-123 implies that very few holes are localized in this compound. The Γ data for underdoped Hg-1201 and Hg-1212 are suppressed relative to that of Hg-1223 and maximally so near $p = 1/8$, consistent with the localization of a fraction of holes.

A similar behavior is seen in the κ data. For $p \leq 0.16$, Hg-1212 has $\kappa(p)$ indistinguishable from that of Hg-1223, except in the narrow range of p near $1/8$ where it is sharply suppressed. κ for Hg-1201 is substantially suppressed over a broader doping range. The implication is that in the absence of localized holes, κ for underdoped Hg-1201 and Hg-1212 would follow the solid curve in Fig. 4(b), an interpolation through a composite of data for all three compounds, excluding the data point at $p \approx 0.18$ for Hg-1223 and ranges of p for Hg-1212 and Hg-1201 where κ is suppressed. The increase in $\kappa(p)$ in the overdoped regime ($p \geq 0.16$) for all compounds is presumably due to the rising κ_e , and possibly to a rising κ_L as well, the latter due, e.g., to a decrease in the phonon-electron scattering.

Our data suggest that the maximum in $\kappa(p)$ observed near $p = 1/8$ for Hg-1223 is an intrinsic feature of κ_L in underdoped cuprates. From kinetic theory, $\kappa_L = 1/3 C_L v^2 \tau$, where C_L is the lattice specific heat, v is the sound velocity, and τ the phonon relaxation time. Interestingly the behavior

of the normal-state elastic constants ($\propto v^2$) of single-crystal La-214 (Ref. 15) parallels that of κ for Hg-1223. A substantial hardening of the lattice in the underdoped regime, with a maximum near $p = x \approx 1/8$, is observed for all symmetries (shear mode data are shown in the inset, Fig. 4). An increasing v^2 is expected quite generally from elastic coupling to conduction electrons for a decreasing electronic density of states (the pseudogap).¹⁶ The appearance of a maximum suggests a competing effect, possibly related to the increasingly magnetic character of the planes. Thus the maximum in κ for underdoped Hg-1223 is plausibly attributed to a renormalized dispersion, and its suppression in compounds with localized holes to increased scattering. In spite of the oversimplification implicit in kinetic theory, these observations suggest that in the absence of localized holes, $\kappa(p)$ for Y-123 would have a similar behavior [solid curve, Fig. 1(a)].

Our interpretation dictates a proportionality between the suppression of κ and Γ , allowing for a self-consistency check. The lattice thermal resistivity ($W \approx 1/\kappa$) introduced by randomly distributed, hole-localized domains should be proportional to their volume fraction since κ is a bulk probe. We then expect Γ (and $\Delta\gamma/\gamma$) to be suppressed by an amount proportional to the same fraction, i.e., $\Delta\Gamma(p) = a\Delta W(p)$, where $\Delta\Gamma$ and ΔW are the amounts by which the measured Γ and W differ from values given by the solid curves in Figs. 1 and 4. This simple relation agrees very well with the data [dashed curves in Figs. 1(b) and 4(b)] using $a^{1212} \approx 1.7$ W/mK, $a^{1201} \approx 2.6$ W/mK, and $a^{Y-123} \approx 2.8$ W/mK.

The Hg data make it clear that oxygen vacancies play only a supporting role in the localization of holes. The importance of $1/8$ doping implies that the phenomenon involves an excitation of the CuO_2 planes that is commensurate with the lattice. A plausible candidate is a small domain of static stripe order,¹ nucleated via pinning by a vacancy-induced mechanism. Recent Raman scattering studies of optimally doped Hg compounds¹⁷ implicate vacancy clusters in pinning: the oscillator strength of the 590 cm^{-1} mode, attributed to c -axis vibrations of apical oxygen in an environment of four vacant nearest-neighbor dopant sites, scales with $\Delta\kappa$ and $\Delta\Gamma$. Oxygen vacancies in both Y-123 and Hg cuprates^{13,18} displace neighboring Ba^{2+} toward the CuO_2 planes. Resulting local distortions of the CuO polyhedra could pin a charge stripe as do the octahedral tilts in (La,Nd)-214.¹ Alternatively, a magnetic mechanism is possible. In the Hg cuprates the shift of Ba atoms associated with a cluster of four vacancies nearest a CuO polyhedron will induce a positive potential in the planes that inhibits its occupation by a hole, thereby suppressing spin fluctuations and possibly fixing a Cu^{2+} spin at the site. Larger vacancy clusters, surrounding adjacent CuO polyhedra oriented along $\langle 100 \rangle$ directions, may induce several spins to order antiferromagnetically via superexchange. The presence of this spin-chain fragment would favor charge or spin segregation that is characteristic of stripe order.

Consider the relevant length scales. If randomly distributed, static stripe domains are to scatter phonons, their in-plane extent must be less than the phonon mean-free-path Λ and their mean separation comparable to Λ . Expressing Λ^{-1} as a sum of terms for scattering by these domains and by all other processes, $\Lambda^{-1} = \Lambda_{\text{str}}^{-1} + \Lambda_{\text{other}}^{-1}$, we use the in-plane

thermal resistivity for Y-123 and kinetic theory to find¹⁹ $\Lambda_{\text{str}} \approx [3/C_L v \Delta W(p=1/8)] \approx 70 \text{ \AA}$ as an estimate of the separation between domains at $p=1/8$. We can make a rough estimate of the fractional area of the planes having static stripes by taking the typical domain size to be $2a \times 8a$ (a is the lattice constant), the stripe unit cell suggested¹ for (La,Nd)-214. This yields a fraction $16(a/\Lambda_{\text{str}})^2 \approx 0.05$. The Γ data suggest that this fraction is somewhat higher in Hg-1201, but apparently below the two-dimensional percolation threshold of 0.50. This presumably explains why no substan-

tial T_c suppression is observed near $p=1/8$ in Y-123 or the Hg cuprates, in contrast to the case of (La,Nd)-124; stripe domains in the latter system have longer-range order ($\geq 170 \text{ \AA}$).¹

The authors acknowledge helpful comments from J. Ashkenazi, S. E. Barnes, M. Peter, and F. Zuo. Work at the University of Miami was supported by NSF Grant No. DMR-9631236, and at the University of Houston by NSF Grant No. DMR-9500625 and the state of Texas through the Texas Center for Superconductivity.

-
- ¹J. M. Tranquada, B. J. Sternlieb, J. D. Axe, Y. Nakamura, and S. Uchida, *Nature (London)* **375**, 561 (1995); J. M. Tranquada, J. D. Axe, N. Ichikawa, A. R. Moodenbaugh, Y. Nakamura, and S. Uchida, *Phys. Rev. Lett.* **78**, 338 (1997).
- ²J. M. Tranquada, *Physica C* **282-287**, 166 (1997); *Physica B* **241-243**, 745 (1998).
- ³P. C. Hammel, B. W. Statt, R. L. Martin, F. C. Chou, D. C. Johnston, and S.-W. Cheong, *Phys. Rev. B* **57**, R712 (1998).
- ⁴P. C. Hammel and D. J. Scalapino, *Philos. Mag.* **74**, 523 (1996); H. Yasuoka, S. Sasaki, T. Imai, T. Shimizu, Y. Ueda, and K. Kosuge, *Phase Transit.* **15**, 183 (1989).
- ⁵J. W. Loram, K. A. Mirza, J. R. Cooper, and W. Y. Liang, *Phys. Rev. Lett.* **71**, 1740 (1993); J. W. Loram, K. A. Mirza, J. R. Cooper, W. Y. Liang, and J. M. Wade, *J. Supercond.* **7**, 243 (1994).
- ⁶B. Battlogg, H. Y. Hwang, H. Takagi, R. J. Cava, H. L. Kao, and J. Kwo, *Physica C* **235-240**, 130 (1994); B. N. Basov, T. Timusk, B. Dabrowski, and J. D. Jorgensen, *Phys. Rev. B* **50**, 3511 (1994); J. L. Tallon, J. R. Cooper, P. S. I. P. N. de Silva, G. V. M. Williams, and J. W. Loram, *Phys. Rev. Lett.* **75**, 4114 (1995); A. Loeser, Z.-X. Shen, D. S. Dessau, D. S. Marshall, C. H. Park, P. Fournier, and A. Kapitulnik, *Science* **273**, 325 (1996); G. V. M. Williams, J. L. Tallon, E. M. Haines, R. Michalak, and R. Dupree, *Phys. Rev. Lett.* **78**, 721 (1997).
- ⁷C. Uher, in *Physical Properties of High Temperature Superconductors*, edited by D. M. Ginsberg (World Scientific, Singapore, 1993), Vol. III, p. 159.
- ⁸C. P. Popoviciu and J. L. Cohn, *Phys. Rev. B* **55**, 3155 (1997); J. L. Cohn, *ibid.* **53**, R2963 (1996).
- ⁹J. L. Tallon, C. Bernhard, H. Shaked, R. L. Hitterman, and J. D. Jorgensen, *Phys. Rev. B* **51**, 12 911 (1995).
- ¹⁰K. Krishana, J. M. Harris, and N. P. Ong, *Phys. Rev. Lett.* **75**, 3529 (1995).
- ¹¹J. L. Cohn, C.-K. Lowe-Ma, and T. A. Vanderah, *Phys. Rev. B* **52**, R13 134 (1995); J. L. Cohn, J. J. Neumeier, C. P. Popoviciu, K. J. McClellan, and Th. Leventouri, *ibid.* **56**, R8495 (1997).
- ¹²Y. J. Uemura, L. P. Le, G. M. Luke, B. J. Sternlieb, W. D. Wu, J. H. Brewer, T. M. Riseman, C. L. Seaman, M. B. Maple, M. Ishikawa, D. G. Hinks, J. D. Jorgensen, G. Saito, and H. Tamochi, *Phys. Rev. Lett.* **66**, 2665 (1991); J. L. Tallon, C. Bernhard, U. Binniger, A. Hofer, G. V. M. Williams, E. J. Ansaldo, J. I. Budnick, and Ch. Niedermayer, *ibid.* **74**, 1008 (1995).
- ¹³O. Chmaissem, Q. Huang, E. V. Antipov, S. N. Putilin, M. Marezio, S. M. Loureiro, J. J. Capponi, J. L. Tholence, and A. Santoro, *Physica C* **217**, 265 (1993); E. V. Antipov, J. J. Capponi, C. Chailloot, O. Chmaissem, S. M. Loureiro, M. Marezio, S. N. Putilin, A. Santoro, and J. L. Tholence, *ibid.* **218**, 348 (1993); Q. Huang, J. W. Lynn, Q. Xiong, and C. W. Chu, *Phys. Rev. B* **52**, 462 (1995).
- ¹⁴Q. M. Lin, Z. H. He, Y. Y. Sun, L. Gao, Y. Y. Xue, and C. W. Chu, *Physica C* **254**, 207 (1996).
- ¹⁵S. Sakita, T. Suzuki, F. Nakamura, M. Nohara, Y. Maeno, and T. Fujita, *Physica B* **219-220**, 216 (1996); M. Nohara, T. Suzuki, Y. Maeno, T. Fujita, I. Tanaka, and H. Kojima, *Phys. Rev. B* **52**, 570 (1995).
- ¹⁶M. Peter and E. R. Walker, *J. Appl. Phys.* **48**, 2820 (1977); B. Lüthi, *J. Magn. Magn. Mater.* **52**, 70 (1985).
- ¹⁷X. Zhou, M. Cardona, C. W. Chu, Q. M. Lin, S. M. Loureiro, and M. Marezio, *Phys. Rev. B* **54**, 6137 (1996).
- ¹⁸J. D. Jorgensen, B. W. Veal, A. P. Paulikas, L. J. Nowicki, G. W. Crabtree, H. Claus, and W. K. Kwok, *Phys. Rev. B* **41**, 1863 (1990).
- ¹⁹We take $C_L(100 \text{ K}) = 1.3 \times 10^6 \text{ J/m}^3\text{K}$ (Ref. 5) and $v = 3 \times 10^3 \text{ m/s}$ estimated from dispersion curves [L. Pintschovius, N. Pyka, W. Reichardt, A. Yu. Rumiantsev, N. L. Mitrofanov, A. S. Ivanov, G. Collin, and P. Bourges, *Physica C* **185-189**, 156 (1991)].